JOURNAL OF APPLIED PHYSICS VOLUME 93, NUMBER 5 1 MARCH 2003

Spin-state effects on the outer core-level multiplet structures for high-spin Mn molecular clusters

A. J. Nelson[a] and John G. Reynolds
Lawrence Livermore National Laboratory, Livermore, California 94550

George Christou
Department of Chemistry, University of Florida, Gainesville, Florida 32611

(Received 8 August 2002; accepted 6 December 2002)

Oxo-bridged manganese polynuclear complexes have applications in a variety of technologies, such as single-molecule nanomagnets, catalysis, and photosynthetic redox chemistry. X-ray photoemission spectroscopy was used to study the Mn $3p$, $3s$, and valence band electronic behavior as a function of Mn cluster structural properties, where the cluster size and nuclearity are systematically varied. Results show a chemical shift of the Mn $3p_{3/2,1/2}$ spin–orbit pair related to the cluster size and nuclearity. In addition, the Mn $3s$ ^{7}S and ^{5}S final state multiplet components shift since they involve the binding energy of a ligand valence electron. In addition, the branching ratio of the ^{7}S:^{5}S states is related to the $3s-3d$ electron correlation. Specifically, in the ^{7}S state, the remaining $3s$ electron is well correlated with $3d$ electrons of parallel spin, while in the ^{5}S state, the two spins are antiparallel. Changes in this electron correlation are clearly observed in the ^{7}S:^{5}S branching ratio as a function of cluster size and ligand electronegativity. *© 2003 American Institute of Physics.* [DOI: 10.1063/1.1540737]

INTRODUCTION

The multiple oxidation states of transition metal ions make them ideally suited for multielectron processes. Clusters of transition metal ions have been found at the active sites of numerous electron transfer enzymes, notably, the tetramanganese cluster in the oxygen-evolving complex, the site of water oxidation in photosynthetic organisms.[1] In addition, Mn=O, where the oxidation state of Mn is +4 or +5, has been identified as the reactive species in catalytic oxidations with Mn porphyrins.[2,3] These catalytic reactions usually end with the complete conversion of the Mn to permanganate, Mn(VII).[4]

Oxo-bridged manganese polynuclear complexes have also proved useful in the development of single-molecule nanomagnets.[5,6] These molecules have a large ground-state spin S, and a large magnetic hysteresis comparable to that observed in hard magnets. This establishes molecular bistability in a molecular nanomagnet, opening the way to store information at the molecular level.

Spin-state effects can be examined by x-ray photoemission spectroscopy (XPS) of outer core-level multiplet structures. Previous photoemission studies on transition metal compounds reveal core-level multiplet structures that are best understood in terms of configuration-interaction (CI) calculations, including intrashell electron correlation, charge-transfer, and final-state screening.[7–11] In addition, these multiplet structures are also strongly influenced by covalency and ligand coordination.[12,13]

The neutral Mn atom has a $1s^2 2s^2 2p^6 3s^2 3p^6 3d^6$ configuration and a high-spin $[3d^5 4s^2]$ configuration. In solids, the (empty) $4s$ band lies 2 to 4 eV above the top of the $3d^N$ band, depending on the ion. Photoelectron transitions are allowed between the initial state $2p^6 3s^2 3p^6 3d^N$ ($N=3,4,5$ for Mn^{+4}, Mn^{+3}, Mn^{+2}, respectively) and a series of final states ($2p^5 3d^{N+1}$).

It has been shown that for Mn dihalides, the outer Mn $3s$ core-level, final-state configuration can be either $3s3d^5$ or $3s3d^6L$ depending on final-state screening effects due to the ligand ($3s$ and L indicate that there is one electron missing in the Mn $3s$ and the ligand valence state, respectively). In addition, the $3s$ final state has ^{7}S and ^{5}S symmetry; for example the Mn^{2+} initial state $(3s^2 3p^6 3d^5)^6$S has two possible final states, $(3s^1 3p^6 3d^5)^7$S or $(3s^1 3p^6 3d^5)^5$S. In the ^{7}S state, the remaining $3s$ electron is well correlated with $3d$ electrons of parallel spin, while in the ^{5}S state, the two spins are antiparallel. This electron correlation reduces the branching ratio of the ^{7}S:^{5}S states. In addition, as the ligand electronegativity decreases, charge-transfer satellites become important, and the spin state purity is lost in the $3s$ spectra. The spectra become representative of mixed unscreened ($3d^N$) and locally screened ($3d^{N+1}$) final states. Thus, we see that the $3s$ core-level is polarized by the $3d^5$ shell.

This article presents the results of a systematic study of the $3s$ and $3p$ core-level photoemission, and satellite structures for Mn oxo-bridged compounds. Outer core-level multiplet splitting was characterized as a function of Mn cluster size, nuclearity, and ligand type. Interpretation of the $3p$ and $3s$ spectra is consistent with the (CI) model, including intrashell electron correlation, charge-transfer, and final-state screening.

EXPERIMENTAL PROCEDURE

The manganese polynuclear complexes have been characterized as having trapped-valence oxidation-state Mn cores

---

[a] Electronic mail: nelson63@llnl.gov

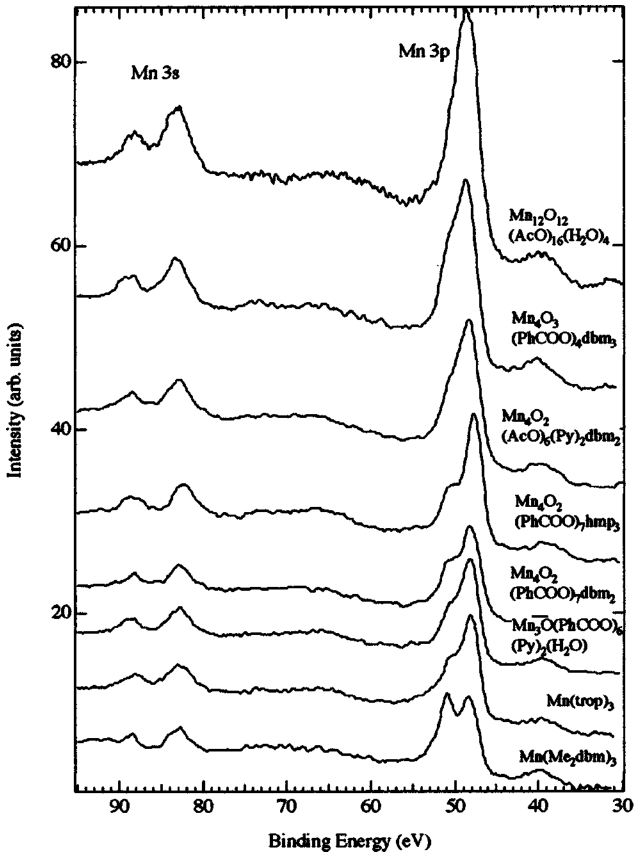

FIG. 1. High-resolution XPS spectra of Mn $3p$ and $3s$ core levels for the Mn polynuclear complexes.

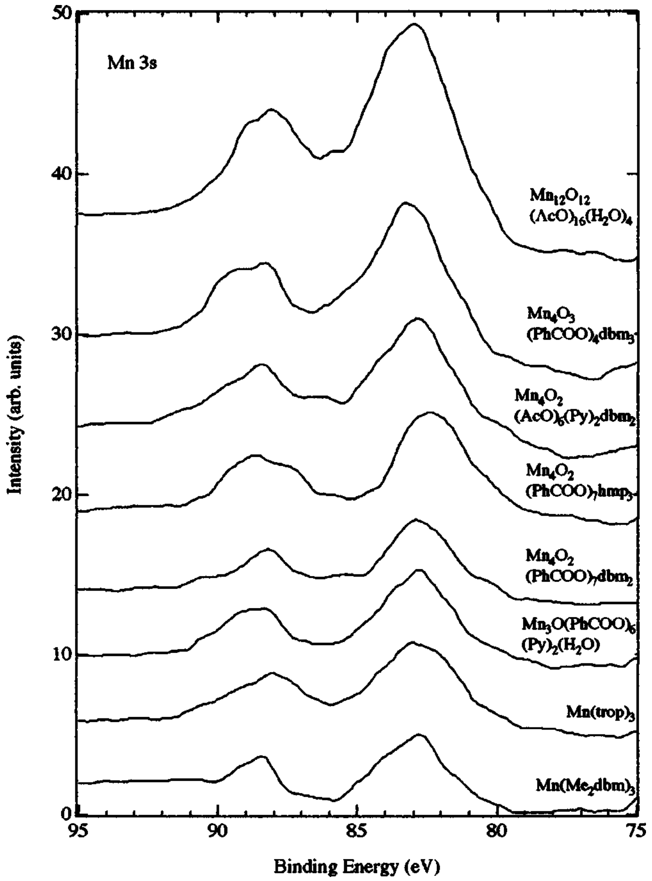

FIG. 2. Expanded high-resolution XPS spectra of Mn $3s$ core levels for the Mn polynuclear complexes.

bridged to various ligands. The Mn cores analyzed are Mn^{3+}, $[Mn_3O]^{6+}$, $[Mn_4O_3]^{7+}$, $[Mn_4O_2]^{8+}$, and $[Mn_{12}O_{12}]^{16+}$. The ligands are the anion of dibenzoylmethane (DBM^-), the anion of 2-hydroxymethyl pyridine (HMP^-), pyridine (Py), and 2-hydroxy-2,4,6-cycloheptatrienone (tropolone or TROP). Note that the ligands $TROP^-$,DBM^- and HMP^- bind as anions, while Py binds as a neutral group. The cation tetra-*n*-butylammonium (TBA) is used as a counter ion. These structures have high ground-state spins, as determined by the oxidation state and topology of the polynuclear transition metal core.[14–16]

Electronic spectroscopy for chemical analysis (ESCA) experiments were performed on a Physical Electronics 5400 ESCA system using Mg K_α radiation (1253.6 eV) and a hemispherical analyzer pass energy of 17.90 eV, giving an overall energy resolution of 1.1 eV. All binding energies are referenced to the Fermi level of the analytical instrument as calibrated to the Au $4f$ peaks. Binding energies were further referenced to the C $1s$ photoelectron line arising from adventitious carbon at 284.6 eV to account for charging effects.

RESULTS AND DISCUSSION

Figure 1 shows the Mn $3s$ and $3p$ spectral regions for the manganese polynuclear complexes. As previously stated, the excitation energy was 1253.6 eV, and thus the positions and relative intensities of the Mn $3s$ and Mn $3p$ multiplets can be considered to be in the sudden limit approximation,[7,8] with little coupling between the ion and the photoelectron. The figure shows a chemical shift of the Mn $3p_{3/2,1/2}$ spin–orbit pair associated with the trapped-valence oxidation states. The unresolved $3p$ peaks are somewhat broadened, but a direct correspondence can be made between observed features in these spectra and those in the literature.[9–11] Specifically, the main $3p$ line represents the ^{7}P ionic final state, and the higher binding energy shoulder represents the spin–orbit component ^{5}P(1). Final-state screening effects in the core-level spectra depend strongly on the electronegativity of the anions (DBM^-, HMP^-, and $TROP^-$) and will affect the final-state branching ratio. Specifically, note the variation of the quintet:septet (^{7}P:^{5}P) final-state branching ratio as the Mn core size increases and becomes a $[Mn_{12}O_{12}]^{16+}$ $8Mn^{III}4Mn^{IV}$ trapped-valence oxidation state. In addition, the covalency of the larger complexes increases, manifesting itself as a drastically reduced $3p$ branching ratio.

Figure 2 presents the expanded Mn $3s$ core-level spectra for the Mn polynuclear complexes. The binding energy positions for the Mn $3s$ ^{7}S and ^{5}S multiplet components are summarized in Table I. Note that the Mn $3s$ multiplet splitting (ΔMn $3s$) becomes smaller as the Mn trapped-valence oxidation state increases, consistent with published data.[7–10] Also note that the ^{7}S and ^{5}S multiplet components shift accordingly since they are correlated with charge transfer between the Mn *d*-states and ligand *p*-states. In addition, note that the full width at half maximum (FWHM) of the ^{5}S mul-

TABLE I. Summary of the Mn 3*p* and 3*s* photoelectron results for manganese polynuclear complexes.

Sample [Mn oxidation state]	Mn 3*p* (eV)		Mn 3*s* (eV)		FWHM of Mn 3*s* peaks (eV)		ΔMn 3*s* (eV)	Mn 3*s* branching ratio[a]
	^{7}P	^{5}P	^{7}S	^{5}S	^{7}S	^{5}S		
$Mn(Me_2DBM)_3$ $[Mn^{III}]$	48.4	50.9 $\Delta=2.5$	82.7	88.4	3.0	1.5	5.7	4.4
$Mn(trop)_3$ $[Mn^{III}]$	48.2	50.2 $\Delta=2.0$	82.7	88.0	3.5	3.2	5.3	1.8
$[Mn_3O(PhCOO)_6$ $(Py)_2(H_2O)]$ $[Mn^{II},2Mn^{III}]$	48.2	50.5 $\Delta=2.3$	82.8	88.6	3.2	2.8	5.8	2.2
$[Mn_4O_2(PhCOO)_7DBM_2]$ TBA $[Mn^{III}]$	48.2	50.4 $\Delta=2.2$	82.9	88.2	2.8	2.0	5.3	2.4
$[Mn_4O_2(PhCOO)_7HMP_3]$ TBA $[Mn^{III}]$	47.7	50.2 $\Delta=2.5$	82.4	88.4	3.0	3.2	6.0	1.8
$[Mn_4O_2(AcO)_6$ $(Py)_2DBM_2]$ $[Mn^{III}]$	48.3	50.6 $\Delta=2.3$	82.8	88.4	3.5	3.0	5.6	2.2
$[Mn_4O_3(PhCOO)_4DBM_3]$ $[3Mn^{III},Mn^{IV}]$	48.7	50.8 $\Delta=2.1$	83.2	88.5	3.2	3.0	5.3	2.1
$[Mn_{12}O_{12}$ $(AcO)_{16}$ $(H_2O)_4]$ $[8Mn^{III},4Mn^{IV}]$	48.7	⋯	83.1	88.2	3.8	4.8	5.1	1.4

[a] The branching ratio of the Mn 3*s* peaks are based the area ratio of the ^{7}S:^{5}S states.

tiplet component is affected by ligand chemistry, consequently affecting the Mn 3*s* branching ratio. Specifically, as the ligand electronegativity decreases, charge-transfer from the ligand *p*-state to the Mn *d*-state causes the spin-state purity to be lost in the 3*s* spectra. Thus, the branching ratio corresponding to $S-1/2$ and $S+1/2$ final states that principally reside on the *p* orbitals of the $[ligand]^-$ and the *d* orbitals of the $[MnO]^+$ core, decreases. Note that the branching ratios for complexes with the DBM ligand are larger since the ^{5}S component is diminished, indicating that the *s*- and *d*-electron spins are mostly parallel.

Figure 3 graphically summarizes the Mn cluster core charge versus Mn 3*s* multiplet splitting for the Mn polynuclear complexes. The multiplet splitting for these ligands is an indication of the 3*s* polarization by the 3*d* final states. In addition, polarization of the ligand can delocalize mobile π electrons and thus affect multiplet splitting.

The polynuclear complex with the largest core size and the $[Mn_{12}O_{12}]^{16+}$ $8Mn^{III}4Mn^{IV}$ trapped-valence oxidation state, exhibits the smallest Mn 3*s* branching ratio. However, this can be affected by the electronic properties of the ligand. Specifically, note that the variation of the Mn 3*s* multiplet splitting for the three complexes with the $[Mn_4O_2]^{8+}$ cores is due to the different ligand electronegativities, the DBM ligand having a higher electronegativity than the HMP ligand. Similarly for the two complexes with Mn^{3+} cores, the $trop^-$ ligand having a higher electronegativity than the Me_2DBM ligand.

CONCLUSIONS

We have presented the results of a systematic study of the 3*s* and 3*p* outer core-level multiplet splitting as a function of Mn cluster size, nuclearity, and ligand type. Results show that the Mn 3*p* final-state branching ratio changes as the Mn core size and trapped-valence oxidation state increases. In addition, as the covalency of the larger complexes increases, the 3*p* branching ratio is reduced. Results also show that the Mn 3*s* multiplet splitting became smaller as the Mn trapped-valence oxidation state increased. The observed multiplet splitting provides further understanding of these oxo-bridged manganese polynuclear complexes.

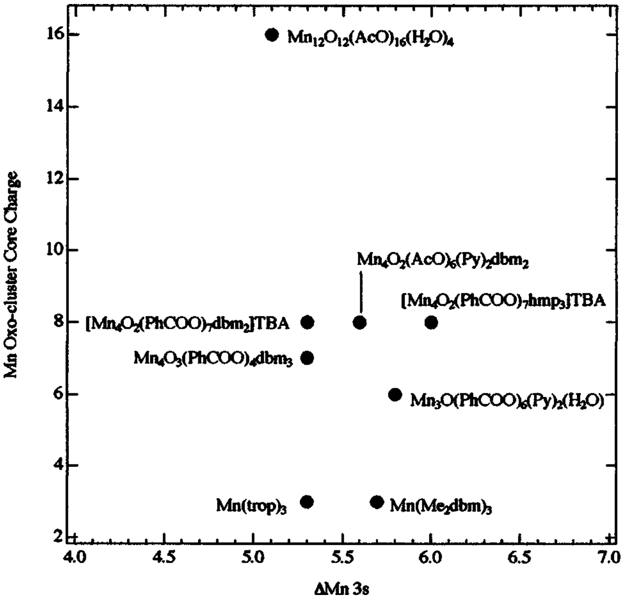

FIG. 3. Mn cluster core charge versus Mn 3*s* multiplet splitting for the Mn polynuclear complexes.

ACKNOWLEDGMENTS

This work was performed under the auspices of the U.S. Department of Energy by University of California, Lawrence Livermore National Laboratory under Contract No. W-7405-ENG-48.

[1] V. K. Yachandra, K. Sauer, and M. P. Klein, Chem. Rev. **96**, 2927 (1996).
[2] J. T. Groves and M. K. Stern, J. Am. Chem. Soc. **110**, 8628 (1988).
[3] J. T. Groves, J. Lee, and S. S. Marla, J. Am. Chem. Soc. **119**, 6269 (1997).
[4] J. Limburg, G. W. Brudvig, and R. H. Crabtree, J. Am. Chem. Soc. **119**, 2761 (1997).
[5] G. Christou, D. Gatteschi, D. N. Hendrickson, and R. Sessoli, MRS Bull. **25**, 66 (2000).
[6] J. Yoo, E. K. Brechin, A. Yamaguchi, M. Nakano, J. C. Huffman, A. L. Maniero, L. C. Brunel, K. Awaga, H. Ishimoto, G. Christou, and D. N. Hendrickson, Inorg. Chem. **39**, 3615 (2000).
[7] P. S. Bagus, A. J. Freeman, and F. Sasaki, Phys. Rev. Lett. **30**, 850 (1973).
[8] C. S. Fadley, in Electron Spectroscopy: *Theory, Techniques, and Applications*, edited by C. R. Brundle and A. D. Baker (Academic, London, 1978), Vol. II, Chap. 1.
[9] B. Hermsmeier, C. S. Fadley, M. O. Krause, J. Jimenez-Mier, P. Gerard, and S. T. Manson, Phys. Rev. Lett. **61**, 2592 (1988).
[10] B. Hermsmeier, C. S. Fadley, B. Sinkovic, M. O. Krause, J. Jimenez-Mier, P. Gerard, T. A. Carlson, S. T. Manson, and S. K. Bhattacharya, Phys. Rev. B **48**, 12425 (1993).
[11] A. von dem Borne, R. L. Johnson, B. Sonntag, M. Talkenberg, A. Verweyen, Ph. Wernet, J. Schulz, K. Tiedtke, Ch. Gerth, B. Obst, P. Zimmermann, and J. E. Hansen, Phys. Rev. A **62**, 052703 (2000).
[12] M. Fujiwara, T. Matsushita, and S. Ikeda, J. Electron Spectrosc. Relat. Phenom. **74**, 201 (1995).
[13] A. J. Nelson, J. G. Reynolds, and J. W. Roos, J. Vac. Sci. Technol. A **18**, 1072 (2000).
[14] M. W. Wemple, H.-L. Tsai, S. Wang, J. P. Cluade, W. E. Streib, J. C. Huffman, D. N. Hendrikson, and G. Christou, Inorg. Chem. **35**, 6437 (1996).
[15] S. Wang, H.-L. Tsai, E. Libby, K. Folting, W. E. Streib, D. N. Hendrikson, and G. Christou, Inorg. Chem. **35**, 7578 (1996).
[16] S. Wang, M. S. Wemple, J. Yoo, K. Folting, J. C. Huffman, K. S. Hagen, D. N. Hendrickson, and G. Christou, Inorg. Chem. **39**, 1501 (2000).